







Steady global surface warming from 1973 to 2022 but increased warming rate after 1990

B. H. Samset ¹✉, C. Zhou ², J. S. Fuglestedt ¹, M. T. Lund ¹, J. Marotzke ^{3,4} & M. D. Zelinka ⁵

The change in global mean surface temperature is a crucial and broadly used indicator of the evolution of climate change. Any decadal scale changes in warming rate are however obfuscated by internal variability. Here we show that the surface temperature increase through the recent La Nina influenced years (2022) is consistent with the 50-year trend of 0.18 °C/decade. We use an Earth System Model based tool to filter out modulations to the warming rate by sea-surface temperature patterns and find consistent warming rates in four major global temperature data series. However, we also find clear indications, in all observational series, of a step-up in warming rate since around 1990. CMIP6 models generally do not capture this observed combination of long-term warming rate and recent increase.

¹CICERO Center for International Climate Research, Oslo, Norway. ²Nanjing University, Nanjing, China. ³Max Planck Institute for Meteorology, Hamburg, Germany. ⁴Center for Earth System Research and Sustainability, Universität Hamburg, Hamburg, Germany. ⁵Lawrence Livermore National Laboratory, Livermore, CA, USA. ✉email: b.h.samset@cicero.oslo.no

The major agencies tracking global surface temperature anomalies (GSTA) rank 2022 as the 5–6th warmest on record^{1–3}. That global warming continues is clear⁴, and apparent in the markedly strengthening impacts felt around the world⁵. Satellites and ocean data also document a strengthening uptake of energy in the Earth system, related to an increasing imbalance between incoming solar radiation and energy re-emitted to space^{6,7}. The recent rate of global mean surface warming—a crucial measure for tracking the progress of climate change and the effects of future mitigation efforts—is however less clear^{8,9}. Primarily, this is due to the influence of internal variability on year-to-year temperature anomalies. 2022 saw strong, prevailing La Niña conditions in the Pacific, which is known to cool the surface, globally, by up to several tenths of a degree Celsius on annual mean. The same was true for 2021, and parts of 2020; an uncommonly long period of cool conditions in the Pacific. This leads to an expectation of observed GSTA values below the full anthropogenic warming since 1850–1900, and an apparent short-term slowdown in the rate of surface warming.

Concurrently, the rate of change, and balance between components of, anthropogenic radiative forcing is also changing⁴. Atmospheric concentrations of CH₄ have increased strongly in the recent decade, while the increase in anthropogenic CO₂ emissions, the primary driver of warming, has slowed to ~1%/year, relative to ~3%/year in the period 1990–2010¹⁰. Emissions of SO₂, precursor of cooling sulfate aerosols, have decreased strongly over the last decade, largely due to strong Chinese efforts to combat air pollution¹¹. Because of the rapid and potentially non-linear influence of aerosol emission changes on surface temperatures⁸, and the remaining uncertainty on the total anthropogenic aerosol forcing of the climate¹², the near-term GSTA evolution can provide a crucial test of the strength of the aerosol-climate interaction. Tracking the rate of change of global surface temperatures is therefore crucial, on both short and long time scales.

Recently, we published a method for filtering out parts of the influence of sea-surface temperature (SST) patterns on the

observed global mean surface temperature anomaly¹³. Briefly, a model-based transfer function is used to relate an SST fluctuation in one location to a global mean effect. This function is in turn applied to the realized, detrended SST pattern for a given month or year, to arrive at a total influence on the GSTA from all ocean areas, which can subsequently be filtered out (Methods). This reduction of the influence of internal variability is an advantage over simple running means, since it includes a physical mechanism linking the SSTs to the GSTA. It is also distinct from common multi-regression approaches that primarily use an ENSO index to quantify ocean variability¹⁴, and from formal detection and attribution techniques as it does not rely on forcing estimates and dedicated simulations.

Applying the method to the HadCRUT5 data series, we found that for the (then) last 50 years (1971–2020), global warming had progressed at an overall rate of 0.19 °C/decade¹³. Here, we update this analysis to include the La Niña influenced years of 2021 and 2022, and show how internal variability has recently affected seasonal and annual global mean temperatures. We then use the method to revisit observed and modelled changes in the rate of global mean surface warming over the last 50-, 20- and 10-year periods.

Results

50-year warming rates. In Fig. 1, we present a breakdown of the SST influence on the GSTA in HadCRUT5, from 1850 and through the last calendar year, including an in-depth look at the last 10 years. The warming influence of the 2016 El Niño is clearly visible, as is the La Niña influence on 2021 and 2022. The annual mean SST related influence on 2021, in our method was found to be -0.09 °C. 2022 was also influenced by the La Niña conditions, but to a lesser degree; we find a cooling of -0.04 °C. For comparison, the El Niño influence in 2016 was $+0.16$ °C. In all, this places 2022 directly on the latest 50-year (1973–2022) trend, which remains at 0.19 ± 0.01 °C/decade. The error is the 5–95%

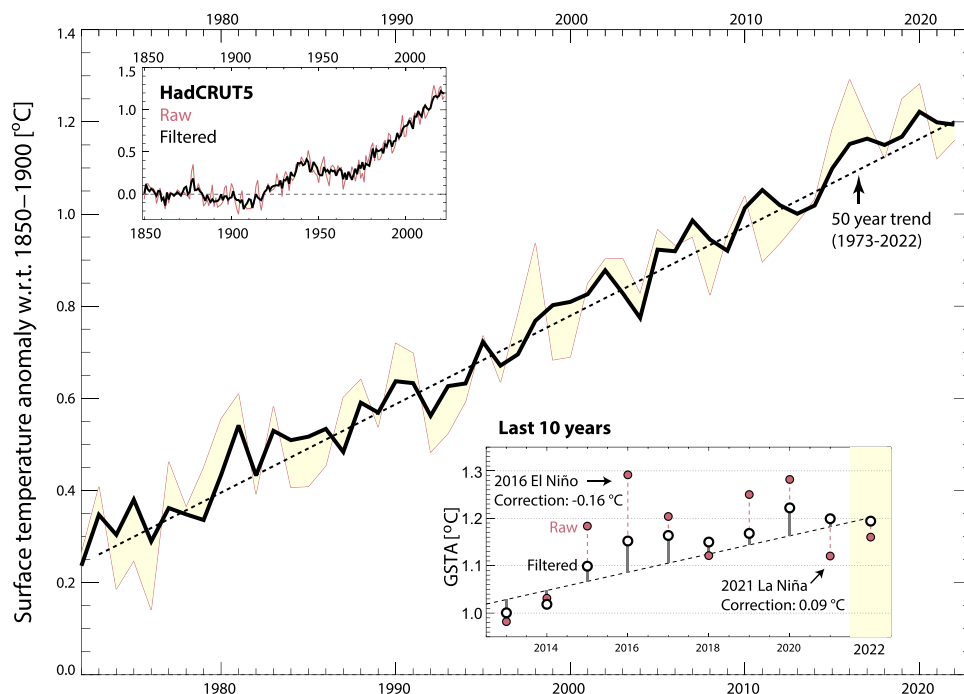


Fig. 1 Steady course for global surface warming for 50 years. All panels show global, annual mean surface temperature anomalies from the HadCRUT5 data series, raw (red) and SST influence filtered via a model derived transfer function (black). The upper and lower insets show, respectively, the full data series since 1850, and the latest 10 years. Anomalies are taken relative to 1850–1899.

Table 1 Global mean surface warming rates for the recent 50-, 20- and 10-year periods, and rate changes calculated using 20-year intervals.

Data series	Filtered			
	Warming rate [°C/decade]			Rate change
	1973–2022	2003–2022	2013–2022	[°C/decade/decade]
HadCRUT5	0.19 ± 0.01	0.21 ± 0.03	0.23 ± 0.08	0.012 ± 0.004
GISTEMP	0.19 ± 0.01	0.23 ± 0.03	0.26 ± 0.06	0.022 ± 0.004
NOAA	0.18 ± 0.01	0.22 ± 0.03	0.25 ± 0.06	0.025 ± 0.003
BEST	0.17 ± 0.01	0.20 ± 0.03	0.24 ± 0.07	0.008 ± 0.003
	Unfiltered			
	Warming rate [°C/decade]			Rate change
	1973–2022	2003–2022	2013–2022	[°C/decade/decade]
HadCRUT5	0.19 ± 0.02	0.21 ± 0.07	0.15 ± 0.25	0.017 ± 0.009
GISTEMP	0.19 ± 0.02	0.22 ± 0.07	0.20 ± 0.26	0.027 ± 0.009
NOAA	0.18 ± 0.02	0.22 ± 0.07	0.17 ± 0.25	0.030 ± 0.009
BEST	0.17 ± 0.02	0.20 ± 0.07	0.17 ± 0.24	0.012 ± 0.010

Numbers are given for filtered and raw global surface temperature anomaly time series. Uncertainties are 5–95% confidence intervals for a linear regression.

confidence interval of the 50-year regression, using the HadCRUT5 ensemble mean.

We also performed the same analysis for three other gridded surface air temperature data products. For the GISTEMP v4, NOAA v5.1 and Berkeley Earth (BEST) surface temperature, we find 50-year warming rates of 0.19, 0.18 and 0.17 °C/decade, respectively. See Table 1. The mean, filtered warming rate of the four series is 0.18 ± 0.01 °C/decade. For recent individual years, all four series give similar results after filtering (see Supplementary Methods 1 and Supplementary Figs. 1–3).

An interesting feature of the filtering method is that it allows us to extract the pattern of ocean temperature influence on the GSTA through a given year. Firstly, we note that the detrended seasonal surface temperature anomalies from HadCRUT5 capture a range of weather events known from news reports of extreme conditions (Supplementary Fig. 4). 2021 began with a cold spell over northern Eurasia, driven by a collapse of the polar vortex, while SSTs are dominated by a very cold Central and Eastern Pacific. This had a strong cooling influence on global surface temperatures in Spring of 2021, albeit counteracted somewhat by a warm fluctuation in the Western Pacific. For 2022, the well documented spring and summer heatwaves in Europe and Asia are apparent, as is a Pacific La Nina pattern that persists through the year. However, other ocean regions had concurrent warm conditions, notably the North Pacific and the Southern Ocean, which counteracted some of the Pacific cooling. An ocean surface hot spot in the Southern Atlantic also contributed to a warmer GSTA toward the end of 2022.

Broadly, we find that anthropogenic global warming is still on a steady course, with recent years tracking near the expectation from the linear 50-year rate (Fig. 1). However, there have been recent discussions, both in the scientific literature^{14,15} and in the public debate, about the possibility of a higher recent rate-of-change of global surface temperature. The increase in Ocean Heat Content (OHC) is also likely to have been accelerating over the last 50 years^{16,17}, which raises the question of whether this change is also reflected in GSTA values.

Warming rate increases since 1990. Table 1 shows warming rates also for the most recent 20- and 10-year periods. After filtering,

these are indeed consistently higher than the 50-year average, consistent with recent literature⁴. In Fig. 2, we investigate this further using filtered data series, updated through 2022, and perform a comparison to CMIP6. Panel a shows filtered GSTA values for the four major data series, with a common, recent baseline (1973–2022). For HadCRUT5, we also show 20-year linear fits at the start and end of the 50-year period. Panel b shows how the regression coefficient of the 20-year fits (in °C/decade) changes with time, for unfiltered and filtered data. Both show an overall increase, as previously documented¹⁵, but the filtered data have a markedly stronger signal-to-noise ratio, of about 1, compared to 0.5 for unfiltered data. A linear regression gives a warming rate increase of 0.012 °C/decade/decade, with a 5–95% confidence interval of [0.008, 0.017]. We also note that the time evolution, with a step-up in rates after 1990, is qualitatively similar to what is found when performing a similar, 20-year sliding window trend analysis on NOAA Ocean Heat Content observations (Supplementary Fig 5).

We now redo this analysis for window lengths of 10–30 years, to see if there is any dependence of the rate increase on the chosen window. Panel c shows the resulting regression coefficients. For all trend windows longer than about 20 years, we find a consistent rate increase for the filtered data. The 5–95% confidence intervals (error bars) also decrease markedly with the length of the fit window, and is strongly reduced by the filtering procedure. The raw data also show an increasing warming rate, but with greater uncertainty and with stronger influence of annual-to-decadal scale internal variability. We also note that the raw data consistently shows a stronger rate increase than the filtered data, indicating differences in the amount of warming filtered through the time period. While the reasons for this require further investigation, it may be due to a systematic shift in SST patterns over the period of study.

Again, similar results are found for the other data series, albeit with different values for rate increases. The GISTEMP, NOAA and BEST surface temperature series yield filtered (20-year window) warming rate increases of 0.022, 0.023 and 0.008 °C/decade/decade, respectively. The mean, filtered warming rate increase of the four series is 0.016 °C/decade/decade. See Table 1, which also shows confidence intervals and unfiltered values. We note that, after filtering, the observational data series are fully consistent in their 50-year warming rates, but inconsistent in their rate increases. This is possibly due to differences in treatment of areas with low observational density, or to differences in their SST data series which map onto the corrections applied by our transfer function.

While we do find a consistent increase in warming rate over the last 50 years, we find no evidence of an “acceleration” of global surface warming in recent years, in the sense of a continuous rate increase. Rather, the strongest increase in rates seems to have occurred as a step-up around the middle of the 50-year period, with a levelling off in later years. This is similar to what is found for OHC (Supplementary Fig 5).

Comparisons to CMIP6. Expectations for near-term warming trends typically come from modelling exercises like CMIP6, using a set of pathways for future emissions and greenhouse gas concentrations. To evaluate any changes in trend, it is therefore of relevance to know if the current model ensemble captures the observed evolution. In Fig. 2 panel d, we compare the 50-year warming rates and rate increases to those from an ensemble of 119 Earth System Model simulations, provided as part of CMIP6 and using historical emissions until 2014, and a Shared Socio-economic Pathway (SSP5–8.5) thereafter. Note that the results are insensitive to the choice of a high or low emission pathway (SSP5–8.5 or SSP1–2.6), as we only extend to 2022 where

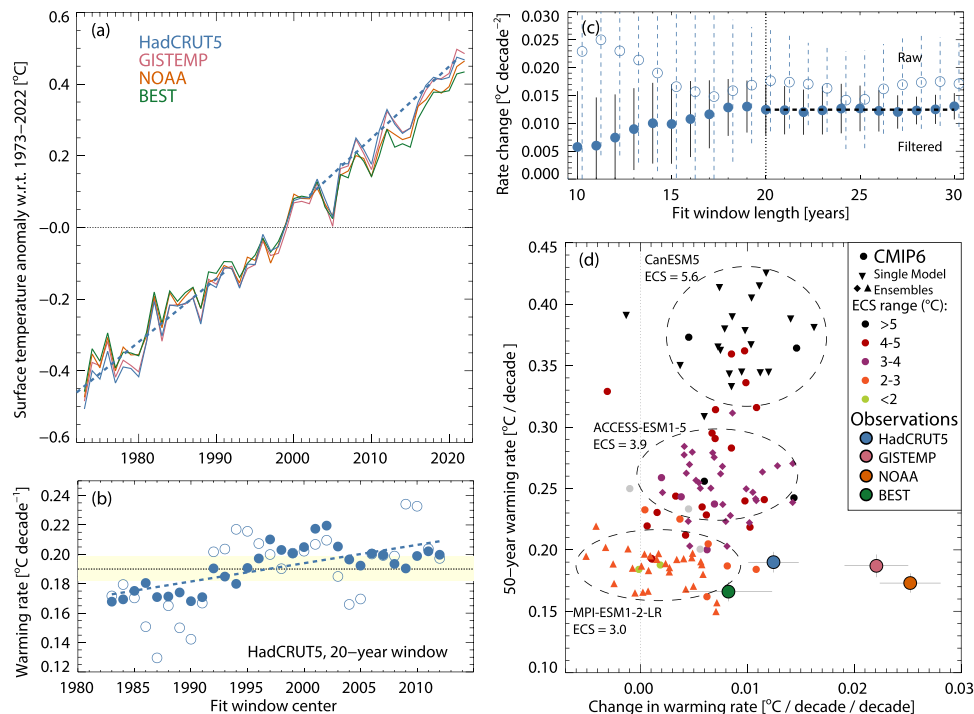


Fig. 2 The rate of global surface warming has been elevated since around 1990. **a** Filtered global surface temperature anomalies for four data series, relative to a common baseline. Dashed lines show 20-year linear regressions for HadCRUT5. **b** Time evolution of rate-of-change of 20-year regressions for HadCRUT5. Open circles show unfiltered data, closed circles show filtered data. The dotted line shows the 50-year warming rate, the yellow box shows the 5–95% confidence interval of the 50-year regression. The dashed line is a linear regression, showing the increase in warming rate over the 50-year period. **c** Warming rate increase (the regression coefficient from the fit in **b**), as function of the length of the fit window, for HadCRUT5. The dotted line shows the 20-year window from **b**. Error bars are 5–95% confidence intervals from the regression. Open circles and dashed lines (offset for clarity) show unfiltered data. **d** 50-year filtered warming rates (y-axis) vs the increase in rate over this period, for four data series (colored circles) and 119 CMIP6 simulations (dots). For CMIP6, the colors indicate the Equilibrium Climate Sensitivity (ECS). Diamonds and triangles show members from three Large Ensembles (CanESM5, ACCESS-ESM1-5, MPI-ESM1-2-LR).

emissions only differ moderately between SSPs. All simulations have been filtered using the transfer function, as for the observations. We show one ensemble member per model, except for three selected models (CanESM5, MPI-ESM1-2-LR and ACCESS-ESM1-5) where we include multiple members to provide an indication of the effects of internal variability. Firstly, virtually all CMIP6 simulations have higher 50-year warming rates than the observations. This result has been discussed in previous literature and is likely due to a combination of high equilibrium climate sensitivities in some CMIP6 models¹⁸, and that the realized SST patterns are not well captured by the model ensemble, notably in the Pacific^{19,20}. We also find a tendency for more rapidly warming models to have a higher rate change over the 50-year period (Fig. 2). These models are generally characterized by higher Equilibrium Climate Sensitivities (ECS) and Transient Climate Responses (TCR; see Supplementary Methods 2 and Supplementary Fig 6). This is particularly clear for the three large ensembles included, which come from models with ECS values ranging from 3.0 °C to 5.6 °C. The observations are notable in that they have higher rate changes than all models of comparable mean warming rates, and generally lie at the upper end of the CMIP6 mean rate change (0.007 °C/decade/decade, calculated using one ensemble member per model). Hence, when looking at warming rate and rate increase in combination, the observations sit well outside the CMIP6 model ensemble. Identifying possible reasons for this requires a broader analysis with other tools than used here, but they may include the poor representation of Pacific SSTs¹⁹, influences of aerosol forcing²¹, and/or the broader climate response to the 1991 eruption of Mt. Pinatubo²².

Discussion

Returning to the near-term evolution of global mean surface temperatures, tracking the global and seasonal evolution of the GSTA for the coming years will clearly give important information on the condition and evolution of the climate system. Firstly, El Niño conditions are projected to develop in late 2023, and last well into 2024. While the strength of the El Niño event is not yet known, when combined with the ongoing rates of change, it can be expected to yield record high GSTA values in 2024. In addition, however, there are still crucial uncertainties remaining about the response of the climate system to continued anthropogenic forcing. One key question is the historical balance between warming from greenhouse gases, notably CO₂ and methane, and cooling from aerosols, notably sulfate²³. While there is a wide spread in possible future aerosol emissions in the Shared Socio-economic Pathways generally used by the climate modelling community²⁴, most scenarios in which emissions are reduced in line with the aims of the Paris Agreement also include strong reductions in aerosol emissions²⁵. The possibility of a very strong aerosol radiative forcing has still not been ruled out. If this is the case, the warming effects aerosol mitigation could rapidly manifest in a change in the rate of global warming.

We therefore advocate for additional attention to, and efforts in tracking, the evolution of the global surface temperature anomaly, when filtered for influence of internal variability. Our conclusion is that global warming continued at a steady rate through 2022, consistent with both longer term 50-year warming rates, and more recent, higher rates. Also, CMIP6 models generally do not reproduce the observed combination of mean

warming rates since 1973, and the recent rate increases, which is concerning for impact studies and climate risk assessments based on these ensembles of simulations. We caution, however, that our conclusions are based on a tool from one model only (Methods), and only take into account sea-surface temperature fluctuations. More sophisticated analyses are possible, using multiple models and also taking into account a wider range of factors such as stratospheric temperatures, volcanic eruptions and the heterogeneous pattern of anthropogenic aerosol emissions, to provide both the scientific community and policy makers with accurate information on the evolution of climate risks over the coming years and decades.

Methods

Datasets. The primary dataset used in this study is the HadCRUT5 gridded dataset of global historical surface temperature anomalies, version 5.0.1.0¹. We used monthly data for the period January 1850–December 2022.

We also used three other gridded surface temperature data products, on monthly resolution, from their start dates and through December 2022: The GISS Surface Temperature Analysis version 4 (GISTEMP v4)^{2,26}, NOAA Global Surface Temperature Dataset (NOAAGlobalTemp) Version 5.1 (updated July 2023), and Berkeley Earth (April 2023 update)²⁷.

Trend removal. The pattern of monthly internal temperature variability is isolated from the long-term influence of anthropogenic warming via a boxcar smoothing with a 10-year window, applied at each grid point of the input dataset, relative to a 1850–1900 baseline. This removes the underlying global mean temperature increase, geographical patterns of global warming, and any seasonal differences. Near the endpoints, where there is insufficient data for the 10-year mean, we ensure consistent weighting by mirroring the data points. This was shown in Samset et al. 2022¹³ to have a negligible impact on the overall results, including trend estimates, even for the end years of the series. Note, however, that our chosen method will not remove decadal scale variability in regional temperature patterns.

Green's functions. The analysis performed is identical to that documented and used in Samset et al. 2022¹³, see that publication for a more thorough writeup and various sensitivity tests and consistency checks. Briefly, we use a Green's Function (GF) calculated with the CESM1.2.1-CAM5.3 Earth System Model, monthly resolved and taking 40-year simulations with fixed sea-surface temperatures as input^{28,29}. A GF, in our usage, relates an idealized increase in sea-surface temperature at a given location, to resulting influences on radiation, clouds, water vapor and, ultimately, global mean surface temperature, and allows us to calculate the modulation of global mean surface temperatures resulting from a given pattern of SST variability. It is based on simulations where the SST was individually perturbed in 74 (partially overlapping) ocean patches of 80° longitude and 40° latitude. We use 2-meter surface air temperature to quantify the modulations.

GSTA modulations are calculated by multiplying the Green's Function for that month with the detrended SST pattern from HadCRUT5. The total modulation is the sum of the contributions from all ocean-dominated grid points. For this calculation, monthly temperature fields from HadCRUT5 and GISTEMP have been regridded to the GF resolution (2.5° latitude, 1.9° longitude).

Climate model data analysis. Climate model simulations shown in Fig. 2 were analyzed identically to the surface data series,

including filtering using the Green's Function. All simulations used were provided for the ScenarioMIP³⁰ CMIP6 Endorsed MIP³¹, and made available to the community through the Earth System Grid Federation (ESGF). We made use of 250-year transient simulations using the CMIP6 historical (1850–2014) and Shared Socioeconomic Pathway (SSP) (2015–2100) emission datasets. Two SSPs were used (SSP1–2.6, SSP5–8.5), to extend the historical data through 2027. (The main analysis runs through 2022, but we use subsequent data so as to avoid the need for mirroring the endpoints). The results of Fig. 2 are insensitive to the choice of SSP (SSP5–8.5, SSP3–7.0, SSP2–4.5, SSP1–2.6). Only monthly mean temperature data (Global Surface Air Temperature at 2 meters) was used. See Supplementary Methods 1 for a list of the 33 individual models and 119 ensemble members used.

Data availability

The processes time series used for the figures in this manuscript, and the underlying analysis, are published on figshare (<https://doi.org/10.6084/m9.figshare.24236434>)³².

The CESM1 Green's Function is documented and made available at <https://github.com/mzmelinka/greens-function> (<https://doi.org/10.5281/zenodo.5514146>).

Surface temperature datasets are publicly available from these websites (accessed on 11.05.2023): <https://www.metoffice.gov.uk/hadobs/hadcrut5/>, <https://data.giss.nasa.gov/gistemp/>, <https://www.ncei.noaa.gov/access/metadata/landing-page/bin/iso?id=gov.noaa.ncdc:C01585>, <https://berkeleyearth.org/data/>.

All climate model simulations used in this paper are publicly available through the ESGF (e.g., <https://esgf-node.llnl.gov/projects/cmip6/>).

NOAA Ocean Heat Content is available from <https://www.ncei.noaa.gov/access/global-ocean-heat-content/>

CMIP6 model ECS and TCR values are available in the Supplementary Information of IPCC AR6 WG1 Chapter 7¹⁶.

Received: 12 June 2023; Accepted: 18 October 2023;

Published online: 01 November 2023

References

- Morice, C. P. et al. An Updated Assessment of Near-Surface Temperature Change From 1850: The HadCRUT5 Data Set. *J. Geophys. Res.: Atmos.* **126**, <https://doi.org/10.1029/2019jd032361> (2021).
- Lenzen, N. J. L. et al. Improvements in the uncertainty model in the Goddard Institute for Space Studies Surface Temperature (GISTEMP) analysis. *J. Geophys. Res.: Atmos.* <https://doi.org/10.1029/2018jd029522> (2019).
- World Meteorological Organization (WMO), State of the Global Climate 2022, WMO-No. 1316, ISBN 978-92-63-11316-0, <https://library.wmo.int/idurl/4/66214> (2023).
- Forster, P. M. et al. Indicators of Global Climate Change 2022: Annual update of large-scale indicators of the state of the climate system and the human influence. *ESDD*, <https://doi.org/10.5194/essd-2023-166> (2023).
- IPCC. Summary for Policymakers [H.-O. Pörtner, et al (eds.)]. In: *Climate Change 2022: Impacts, Adaptation and Vulnerability. Contribution of Working Group II to the Sixth Assessment Report of the Intergovernmental Panel on Climate Change* [H.-O. Pörtner, D.C. Roberts, M. Tignor, E.S. Poloczanska, K. Mintenbeck, A. Alegria, M. Craig, S. Langsdorf, S. Löschke, V. Möller, A. Okem, B. Rama (eds.)]. Cambridge University Press, Cambridge, UK and New York, NY, USA, <https://doi.org/10.1017/9781009325844.00> (2022).
- Loeb, N. G. et al. Satellite and Ocean Data Reveal Marked Increase in Earth's Heating Rate. *Geophysical Research Letters* **48**, <https://doi.org/10.1029/2021gl093047> (2021).
- von Schuckmann, K. et al. Heat stored in the Earth system 1960–2020: where does the energy go? *Earth System Sci. Data* **15**, 1675–1709 (2023).
- Samset, B. H., Fuglestad, J. S. & Lund, M. T. Delayed emergence of a global temperature response after emission mitigation. *Nat. Commun.* **11**, 3261 (2020).
- McKenna, C. M., Maycock, A. C., Forster, P. M., Smith, C. J. & Tokarska, K. B. Stringent mitigation substantially reduces risk of unprecedented near-term warming rates. *Nat. Clim. Change* **11**, 126–131 (2020).
- Friedlingstein, P. et al. Global Carbon Budget 2022. *Earth Syst. Sci. Data* **14**, 4811–4900 (2022).
- Zheng, Y., Zhang, Q., Tong, D., Davis, S. J. & Caldeira, K. Climate effects of China's efforts to improve its air quality. *Environ. Res. Lett.* **15**, <https://doi.org/10.1088/1748-9326/ab9e21> (2020).

12. Bellouin, N. *et al.* Bounding Global Aerosol Radiative Forcing of Climate Change. *Rev. Geophys.* **58**, <https://doi.org/10.1029/2019rg000660> (2020).
13. Samset, B. H. *et al.* Earlier emergence of a temperature response to mitigation by filtering annual variability. *Nat. Commun.* **13**, 1578 (2022).
14. Foster, G. & Rahmstorf, S. Global temperature evolution 1979–2010. *Environ. Res. Lett.* **6**, <https://doi.org/10.1088/1748-9326/6/4/044022> (2011).
15. Richardson, M. T. Prospects for Detecting Accelerated Global Warming. *Geophys. Res. Lett.* **49**, <https://doi.org/10.1029/2021gl095782> (2022).
16. Forster, P. *et al.* in *Climate Change 2021: The Physical Science Basis. Contribution of Working Group I to the Sixth Assessment Report of the Intergovernmental Panel on Climate Change* (eds Masson-Delmotte, V. *et al.*) 923–1054 (Cambridge University Press, 2021).
17. Cheng, L., Foster, G., Hausfather, Z., Trenberth, K. E. & Abraham, J. Improved Quantification of the Rate of Ocean Warming. *J. Clim.* **35**, 4827–4840 (2022).
18. Zelinka, M. D. *et al.* Causes of Higher Climate Sensitivity in CMIP6 Models. *Geophys. Res. Lett.* **47**, <https://doi.org/10.1029/2019gl085782> (2020).
19. Seager, R. *et al.* Strengthening tropical Pacific zonal sea surface temperature gradient consistent with rising greenhouse gases. *Nat. Clim. Change* **9**, 517–522 (2019).
20. Wills, R. C. J., Dong, Y., Proistosescu, C., Armour, K. C. & Battisti, D. S. Systematic Climate Model Biases in the Large-Scale Patterns of Recent Sea-Surface Temperature and Sea-Level Pressure Change. *Geophys. Res. Lett.* **49**, <https://doi.org/10.1029/2022gl100011> (2022).
21. Smith, C. J. & Forster, P. M. Suppressed Late-20th Century Warming in CMIP6 Models Explained by Forcing and Feedbacks. *Geophys. Res. Lett.* **48**, <https://doi.org/10.1029/2021gl094948> (2021).
22. Fyfe, J. C. *et al.* Making sense of the early-2000s warming slowdown. *Nat. Clim. Change* **6**, 224–228 (2016).
23. Eyring, V. *et al.* Human Influence on the Climate System. In *Climate Change 2021: The Physical Science Basis. Contribution of Working Group I to the Sixth Assessment Report of the Intergovernmental Panel on Climate Change* [eds Masson-Delmotte, V., Zhai, P., Pirani, A., Connors, S. L., Péan, C., Berger, S., Caud, N., Chen, Y., Goldfarb, L., Gomis, M. I., Huang, M., Leitzell, K., Lonnoy, E., Matthews, J.B.R., Maycock, T.K., Waterfield, T., Yelekçi, O., Yu, R. and Zhou, B.]. 423–552 (Cambridge University Press, Cambridge, United Kingdom and New York, NY, USA, 2021).
24. Lund, M. T. *et al.* A continued role of short-lived climate forcings under the Shared Socioeconomic Pathways. *Earth Syst. Dyn.* **11**, 977–993 (2020).
25. Riahi, K. *et al.* Mitigation pathways compatible with long-term goals. In *IPCC, 2022: Climate Change 2022: Mitigation of Climate Change. Contribution of Working Group III to the Sixth Assessment Report of the Intergovernmental Panel on Climate Change* [eds Shukla, P.R., Skea, J., Slade, R., Al Khouradajie, A., van Diemen, R., McCollum, D., Pathak, M., Some, S., Vyas, P., Fradera, R., Belkacemi, M., Hasija, A., Lisboa, G., Luz, S., Malley, J.]. Cambridge University Press, Cambridge, UK and New York, NY, USA. <https://doi.org/10.1017/9781009157926.005> (2022).
26. Team, G. *GISS Surface Temperature Analysis (GISTEMP), version 4*, <<https://data.giss.nasa.gov/gistemp/>> (2023).
27. Rohde, R. A. & Hausfather, Z. The Berkeley Earth Land/Ocean Temperature Record. *Earth Syst. Sci. Data* **12**, 3469–3479 (2020).
28. Zhou, C., Zelinka, M. D. & Klein, S. A. Analyzing the dependence of global cloud feedback on the spatial pattern of sea surface temperature change with a Green's function approach. *J. Adv. Modeling Earth Syst.* **9**, 2174–2189 (2017).
29. Zhou, C., Lu, J., Hu, Y. & Zelinka, M. D. Responses of the Hadley Circulation to Regional Sea Surface Temperature Changes. *J. Clim.* **33**, 429–441 (2020).
30. O'Neill, B. C. *et al.* The Scenario Model Intercomparison Project (ScenarioMIP) for CMIP6. *Geosci. Model Dev.* **9**, 3461–3482 (2016).
31. Eyring, V. *et al.* Overview of the Coupled Model Intercomparison Project Phase 6 (CMIP6) experimental design and organization. *Geosci. Model Dev.* **9**, 1937–1958 (2016).
32. Samset, B. H. *et al.* <https://doi.org/10.6084/m9.figshare.24236434> (Figshare, 2023).

Acknowledgements

We thank Ed Hawkins and Laura Wilcox for good input to the paper during its preparation. B.H.S., J.S.F., and M.T.L. acknowledge funding by the Research Council of Norway through projects CATHY (324182), and internal funding from CICERO Center for International Climate Research. The work of M.D.Z. was supported by the U.S. Department of Energy (DOE) Regional and Global Model Analysis program area and was performed under the auspices of the DOE by Lawrence Livermore National Laboratory under Contract DE-AC52-07NA27344. J.M. was supported by the Max Planck Society for the Advancement of Science. The work of CZ was supported by the National Natural Science Foundation of China (Grant No. NSFC 41875095 and 42075127).

Author contributions

B.H.S. conceived and designed the study, and performed the analysis. C.Z. and M.D.Z. produced and provided the GFs. B.H.S., C.Z., J.S.F., M.T.L., J.M., and M.D.Z. all contributed to shaping the conclusions, discussing and testing the methods, and writing the paper.

Competing interests

The authors declare no competing interests.

Additional information

Supplementary information The online version contains supplementary material available at <https://doi.org/10.1038/s43247-023-01061-4>.

Correspondence and requests for materials should be addressed to B. H. Samset.

Peer review information *Communications Earth & Environment* thanks Karsten Haustein and the other, anonymous, reviewer(s) for their contribution to the peer review of this work. Primary Handling Editors: Heike Langenberg. A peer review file is available.

Reprints and permission information is available at <http://www.nature.com/reprints>

Publisher's note Springer Nature remains neutral with regard to jurisdictional claims in published maps and institutional affiliations.



Open Access This article is licensed under a Creative Commons Attribution 4.0 International License, which permits use, sharing, adaptation, distribution and reproduction in any medium or format, as long as you give appropriate credit to the original author(s) and the source, provide a link to the Creative Commons license, and indicate if changes were made. The images or other third party material in this article are included in the article's Creative Commons license, unless indicated otherwise in a credit line to the material. If material is not included in the article's Creative Commons license and your intended use is not permitted by statutory regulation or exceeds the permitted use, you will need to obtain permission directly from the copyright holder. To view a copy of this license, visit <http://creativecommons.org/licenses/by/4.0/>.

© The Author(s) 2023